International Journal of Heat and Mass Transfer 106 (2017) 720–730

Contents lists available at ScienceDirect

International Journal of Heat and Mass Transfer

journal homepage: www.elsevier.com/locate/ijhmt

Effect of electromagnetic field on distribution of temperature, velocity and concentration during saturated flow in porous media based on Local Thermal Non-Equilibrium models (influent of input power and input velocity)

Prempreeya Montienthong [a], Phadungsak Rattanadecho [a,*], Waraporn Klinbun [b]

[a] Department of Mechanical Engineering, Faculty of Engineering, Thammasat University (Rangsit Campus), 99 Moo 18, Klong Luang, Pathumthani 12120, Thailand
[b] Panyapiwat Institute of Management, 85/1 Moo 2, Chaengwattana Rd., Bang Talad, Pakkred, Nonthaburi 11120, Thailand

ARTICLE INFO

Article history:
Received 11 May 2016
Received in revised form 17 September 2016
Accepted 18 September 2016
Available online 27 September 2016

Keywords:
Darcy–Brinkman–Forchheimer's model
Distribution of concentration
Electromagnetic field (mode TE_{10})
Local Thermal Non Equilibrium (LTNE) models

ABSTRACT

The work presents the effect of electromagnetic field on distribution of temperature, velocity and concentration during saturated flow in porous media. The simulations of electromagnetic field (mode TE_{10}) are obtained by solving Maxwell's equations via the finite difference time domain method (FDTD). In addition, Darcy–Brinkman–Forchheimer's model are used to describe the pattern of fluid flow and intensity distribution in porous media where the finite control volume model and SIMPLE algorithm are used to solve these system of equations. The two energy equations for solid and fluid phases are proposed in model of Local Thermal Non Equilibrium condition (LTNE). The effects of input power of electromagnetic wave i.e. 500, 800 and 1600 W, input velocity i.e. Re_p 0.1, 0.5 and 10 were investigated. Distribution of temperature, velocity field and concentrated contaminants in transferred fluid inside of porous media were discussed. The results have also shown major issues on how high power of electromagnetic wave, significantly affects the distribution of temperature, concentration and the velocity field.

1. Introduction

Microwaves have an important role in industry. The advantages of producing heat from microwave are high efficiency, the ability to select receiving heat, and energy penetration, which causes the heat to be distributed uniformly through the object. Usually, heat transfer in porous media such as means some examples, such as boiled eggs in salt water, oil on the beach, or impurities in water that has been heated by the sun. All these porous materials with contaminants are heated under forced convection and natural convection. Applications of electromagnetic waves are widely implemented in food industry and packaging in microwave food. Thermal natural convection combined with electromagnetic waves in porous media is normally seen in environments such as the movement of water in geothermal reservoirs, underground spreading of chemical wastes and other pollutants, grain storage, thermal insulation, evaporative cooling and solidification [1]. Concentration or mass diffusion in porous media is frequently found in daily life, for example in the infiltration of contaminants and fertilizer through soil layers, contaminants in food, catalytic converters in cars and crystal growth. One of the applications of mass diffusion or concentration is the sintering process – the process of heating a material to just below the melting point so that it forms one solid mass to create a solid material such as metal and ceramic powders, and so on [2].

Karimi-Fard et al. [2] carried out a numerical study of double-diffusive natural convection in a square cavity filled in porous media. This research focused on the influence of the Lewis number on the inertial and boundary effects which affected the double-diffusive convection. Khanafer and Vafai [1] presented a numerical study of mixed-convection heat and mass transport in a lid-driven square enclosure which was filled in a non-Darcian fluid-saturated porous medium. The results were that the buoyancy ratio, Darcy number, Lewis number, and Richardson number had profound effects on the double-diffusive phenomenon. Jena et al. [3] presented a study that focused on analyzing the buoyancy opposed double diffusive natural convection in a square porous cavity having partially active thermal and solutal walls. Trevisan and Bejan [4] studied the natural convection phenomenon occurring inside a porous layer with both heat and mass transfer from the side. The natural circulation was driven by a combination of buoyancy

* Corresponding author.
E-mail address: ratphadu@engr.tu.ac.th (P. Rattanadecho).

http://dx.doi.org/10.1016/j.ijheatmasstransfer.2016.09.059
0017-9310/

Nomenclature

A	area (m^2)
C_p	specific heat capacity (J/kg K)
D_p	penetration depth (m)
E	electric field (V/m)
f	electromagnetic wave frequency (Hz)
H	magnetic field strength (A/m)
h	heat transfer coefficient (W/m^2 K)
P	power (W)
Q	heat generation term (W/m^3)
Re_p	particle Reynolds number, $\rho_f u_e d_p/\mu$
T	temperature (°C)
$\tan\delta$	loss tangent
t	time (s)
u, v	velocity (m/s)

Greek letters

ε	porosity
ρ	density (kg m^{-3})
β_T	coefficient of thermal expansion
β_C	coefficient of concentration expansion
ϕ	magnetic permeability (h/m)
ω	angular frequency (rad/s)
σ	electric conductivity (W m^{-1} K^{-1})
γ_0	dielectric constant
γ'_r	relative dielectric constant
γ''_r	relative dielectric loss factor

Subscripts

f	fluid
s	solid
x, y, z	coordinate

effects with temperature and concentration variations. Nishimura et al. [5] showed the effect of the buoyancy ratio on the flow structure which was investigated numerically for a binary mixture gas in a rectangular enclosure. Weaver and Viskanta [6] presented the influence of augmenting and opposing thermal and solutal buoyancy forces on natural convection in binary gases. Nithiarasu et al. [7] demonstrated double-diffusive natural convective flow within a rectangular enclosure.

Heat and mass transfers in microwave heating processes, including natural convection in liquids, have been investigated. Saltiel and Datta [8] investigated heat transfer in liquid at any point of the solid and fluid temperature by using the Local Thermal Equilibrium (LTE) model.

Investigations of heat transfer in microwave heating processes and natural convection in porous media are complicated. Many researchers have attempted to study this problem. Wessapan and Rattanadecho [9] carried out a numerical analysis of the specific absorption rate (SAR) and the heat transfer in a heterogeneous two-dimensional human eye model exposed to the TM-mode of electromagnetic (EM) fields of 900 MHz at various power densities. Cha-um et al. [10] presented the process of heating dielectric materials by microwave with a rectangular waveguide. The results show that the locations of sample have greater effects than the other parameters. Klinbun et al. [11] presented a numerical and experimental analysis of microwave heating in a saturated packed bed by using a rectangular waveguide (TE_{10} mode), where the mathematical is based on the LTE model.

Previous researches are based on invoking the LTE model based on the assumption that the solid phase temperature is equal to the fluid phase temperature everywhere in the porous media. Two different models are used for analyzing heat transfer in a porous media, that is, the LTE and the Local Thermal Non-Equilibrium (LTNE) model. In recent years, the LTNE model has received more attention in demonstrating heat transport in porous media because the LTE model is not suitable for a number of physical situations such as fluid flows at high speed through porous media.

Heat transfer in microwave heating processes and natural convection in porous media under the LTNE were studied by Keangin and Rattanadecho [12]. The influences of blood velocities, porosities, input microwave powers and positions within the porous liver on the tissue and blood temperature distributions have been investigated.

Klinbun et al. [13] also studied heat transfer in microwave heating processes and forced convection in porous media under the LTNE model. The effect of an electromagnetic field on forced convection in a fluid-saturated porous medium was analyzed. The effects of the dimensionless electromagnetic wave power and dimensionless electromagnetic wave frequency on the dimensionless temperature field and Nusselt number distribution are discussed. This research found temperature and Nusselt number values increase substantially with an increase in the electromagnetic power.

In the same way, Nakayama et al. [14], Quintard [15], Amiri and Vafai [16] and Kuznetzov [17] also researched the heat transfer in porous media by using the LTNE model, but the difference in microwave is not related to their research.

It seems that the LTE model does not consider the temperature difference between the solid and fluid phases within the porous media, but this temperature difference has a significant influence on the heat transfer. Therefore, for this research, the LTNE model was chosen to analyze the effect of an electromagnetic field on the distribution of temperature, velocity, and concentration during saturated flow in a porous media.

However, a few studies concentrated energy equations, momentum and concentration equations of porous media subjected to electromagnetic fields under the LTNE model. Therefore, to approach reality, modeling of heat transport, momentum and concentration in porous media must cooperate with the modeling of the electromagnetic field in order to complete this analysis. In addition, there are various effects related to the solid and fluid temperatures and the flow field, such as the input velocities and input microwave powers, that are still not well understood.

In this study, the distributions of solid and fluid temperatures, concentration, and flow field within a porous media under electromagnetic wave are investigated based on the LTNE model. The distribution of temperature, velocity field, and concentrated contaminants during saturated flow in the porous media are discussed. Mathematical model of the porous media approach is proposed; it uses transient energy, momentum, and concentration equations coupled with Maxwell's equation. The coupled nonlinear set of governing equations as well as the initial and boundary conditions is solved using the finite control volume and finite difference time domain method.

2. Analysis

Saturated flow through a packed bed of spherical particles subjected to an electromagnetic field as shown in Fig. 1 is considered.

The configuration consists of a porous media that fills inside a rectangular waveguide. The assumptions are as follows. Walls of the guide are assumed to be made of metal which approximates a perfect electrical conductor. The monochromic wave in fundamental mode (TE_{10}) is applied in the x-direction. The domain in which the electromagnetic field is analyzed includes the entire region enclosed by the walls of the guide. For temperature and flow fields the computational domain is limited to the region enclosed by the container. The horizontal walls of container are kept at a constant temperature.

2.1. Analysis of the electromagnetic field

Maxwell's equations for TE_{10} mode are solved to obtain the electromagnetic field inside a rectangular waveguide and the enclosed porous medium [13].

$$E_z,\ H_x,\ H_y \neq 0 \tag{1}$$

$$\frac{\partial E_z}{\partial t} = \frac{1}{\gamma}\left(\frac{\partial H_y}{\partial x} - \frac{\partial H_x}{\partial y} - \sigma E_z\right) \tag{2}$$

$$\frac{\partial H_x}{\partial t} = -\frac{1}{\varphi}\left(\frac{\partial E_z}{\partial y}\right) \tag{3}$$

$$\frac{\partial H_y}{\partial t} = \frac{1}{\varphi}\left(\frac{\partial E_z}{\partial x}\right) \tag{4}$$

where E and H are the electric and magnetic fields, γ is electric permittivity, φ is magnetic permeability, and σ is electric conductivity.

2.1.1. Boundary and initial conditions

(1) Perfect conduction condition is utilized at the inner walls surface of waveguide. Therefore, normal components of the magnetic field and tangential components of the electric field vanish at these walls:

$$H_n = 0,\ E_t = 0 \tag{5}$$

where subscripts t, n denote the components of tangential and normal directions, respectively.

(2) The first order absorbing condition by Mur [18] are used at the both ends of the waveguide:

$$\frac{\partial E_x}{\partial t} = \pm c\frac{\partial E_x}{\partial x} \tag{6}$$

where is $\pm$ represented forward and backward direction and is denotes the phase velocity of the propagation wave.

(3) The input microwave source is simulated by the equations [13]:

$$E_z = E_{zin}\sin\left(\frac{\pi y}{a}\right)\sin(2\pi f t) \tag{7}$$

$$H_y = \frac{E_{zin}}{Z_H}\sin\left(\frac{\pi y}{a}\right)\sin(2\pi f t) \tag{8}$$

where f is the frequency of microwave, y is the width of the rectangular waveguide, Z_H is the wave impedance, E_{zin} and is the input value of the electric field intensity. By applying the Poynting theorem, the input value of the electric field intensity is evaluated by the microwave power input as:

$$E_{zin} = \sqrt{\frac{4Z_H P_{in}}{A}} \tag{9}$$

where P_{in} is the microwave power input and A is the area of the incident plane.

(4) The continuity conditions at the interface between different materials are given by:

$$E_t = E'_t,\quad H_t = H'_t \tag{10}$$

$$D_n = D'_n,\quad B_n = B'_n \tag{11}$$

(5) Initial conditions:

$$E,\ H = 0 \quad ;t = 0 \tag{12}$$

2.2. Analysis of flow, temperature field and concentration

To reduce the complicate of the problem, the following assumptions are applied:

(1) The fluid is an incompressible Newtonian fluid.
(2) Phase change does not occur.
(3) The Boussinesq approximation is applied.
(4) The porous medium is isotropic.
(5) The effect of magnetic field on heating is negligible.
(6) Thermal dispersion is omitted.

The governing equations for analysis flow and heat transfer in this study areas following:

Continuity equation:

$$\frac{\partial u}{\partial x} + \frac{\partial v}{\partial y} = 0 \tag{13}$$

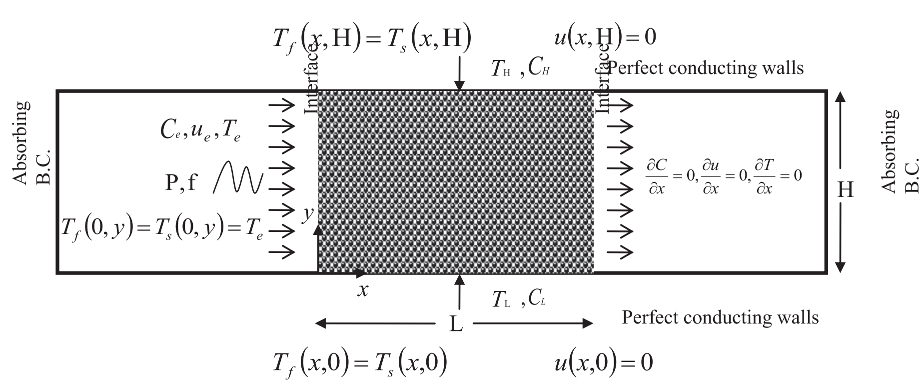

Fig. 1. Schematic diagram of the problem under consideration and the corresponding coordinate system.

Momentum equation:

$$\frac{1}{\varepsilon}\left(\frac{\partial u}{\partial t}\right)+\frac{1}{\varepsilon^2}\left(u\frac{\partial u}{\partial x}+v\frac{\partial u}{\partial y}\right)=-\frac{1}{\rho_f}\left(\frac{\partial p}{\partial x}\right)+\frac{\mu}{\varepsilon}\left(\frac{\partial^2 u}{\partial x^2}+\frac{\partial^2 u}{\partial y^2}\right)-\frac{\mu u}{\kappa}-\frac{F\mu}{\sqrt{\kappa}}(u^2+v^2)^{1/2}u \tag{14}$$

$$\frac{1}{\varepsilon}\left(\frac{\partial v}{\partial t}\right)+\frac{1}{\varepsilon^2}\left(u\frac{\partial v}{\partial x}+v\frac{\partial v}{\partial y}\right)=-\frac{1}{\rho_f}\left(\frac{\partial p}{\partial y}\right)+\frac{\mu}{\varepsilon}\left(\frac{\partial^2 v}{\partial x^2}+\frac{\partial^2 v}{\partial y^2}\right)-\frac{\mu v}{\kappa}-\frac{F\mu}{\sqrt{\kappa}}(u^2+v^2)^{1/2}v+g\beta_T(T-T_0)+g\beta_C(C-C_0) \tag{15}$$

The geometric function, F and permeability, κ [13]

$$F=\frac{1.75}{\sqrt{150\varepsilon^3}} \tag{16}$$

$$\kappa=\frac{\varepsilon^3 d_p^2}{150(1-\varepsilon)^2} \tag{17}$$

In addition, the variation of porosity near the impermeable boundaries can be expressed as [13].

$$\varepsilon=\varepsilon_\infty\left[1+a_1\exp\left(-\frac{a_2 y}{d_p}\right)\right]\quad a_1, a_2 \text{ are empirical constants} \tag{18}$$

Fluid phase energy equation:

$$\varepsilon(\rho C_p)_f\frac{\partial T_f}{\partial t}+(\rho C_p)_f\left(u\frac{\partial T_f}{\partial x}+v\frac{\partial T_f}{\partial y}\right)=k_{feff}\left(\frac{\partial^2 T_f}{\partial x^2}+\frac{\partial^2 T_f}{\partial y^2}\right)+h_{sf}a_{sf}(T_s-T_f)+\varepsilon Q_f \tag{19}$$

Solid phase energy equation:

$$(1-\varepsilon)(\rho C_p)_s\frac{\partial T_s}{\partial t}=k_{seff}\left(\frac{\partial^2 T_s}{\partial x^2}+\frac{\partial^2 T_s}{\partial y^2}\right)-h_{sf}a_{sf}(T_s-T_f)+(1-\varepsilon)Q_s \tag{20}$$

where Q is the local electromagnetic heat generation term, which is a function of the electric field and defined as:

$$Q=2\pi f\gamma_0\gamma_r'(\tan\delta)\cdot(E_z)^2 \tag{21}$$

$$\tan\delta=\frac{\gamma_r''}{\gamma_r'}=\frac{\sigma}{\omega\gamma_r'\gamma_0} \tag{22}$$

Concentration equation:

The concentration transport equation is utilized [1,2]

$$\varepsilon\frac{\partial C}{\partial t}+u\frac{\partial C}{\partial x}+v\frac{\partial C}{\partial y}=D\left(\frac{\partial^2 C}{\partial x^2}+\frac{\partial^2 C}{\partial y^2}\right) \tag{23}$$

Boundary and initial conditions:

From Fig. 1, no slip boundary conditions are applied at all the solid walls which are kept at a constant temperature. Thus, the boundary conditions are as follows:

$$T_f(0,y)=T_s(0,y)=T_e=27\,^\circ\mathrm{C}$$
$$T_f(x,\mathrm{H})=T_s(x,\mathrm{H})=T_\mathrm{H}=67\,^\circ\mathrm{C}$$
$$T_f(x,0)=T_s(x,0)=T_\mathrm{L}=15\,^\circ\mathrm{C}$$
$$u(0,y)=u_e,\ \mathrm{Re_p}=\rho_f u_e d_p/\mu$$
$$u(x,\mathrm{H})=0$$
$$u(x,0)=0$$
$$C(0,y)=C_e=30,\ 0.03\ \mathrm{mol/dm^3}$$
$$C(x,\mathrm{H})=C_\mathrm{H}=20\ \mathrm{mol/dm^3}$$
$$C(x,0)=C_\mathrm{L}=10\ \mathrm{mol/dm^3}$$

From Fig. 1, Outlet boundary conditions are used for model flow exits where the details of the flow velocity and pressure are not known prior to solution of the flow problem. There are appropriate where the exit flow is close to a fully developed condition, as the outlet boundary condition assumes a zero normal gradient for all flow variables except pressure.

$$\frac{\partial C}{\partial x}=0,\quad \frac{\partial u}{\partial x}=0,\quad \frac{\partial T}{\partial x}=0.$$

Initial conditions are as follows:

$$T=T_0=27\,^\circ\mathrm{C}$$
$$u=u_0$$
$$C=C_0=0\ \mathrm{mol/dm}^{\ 3};\ t=0$$

The Dielectric and thermal properties are listed in Table 1 [13].

3. Numerical simulations

Maxwell's equations are solved using the finite-difference time-domain (FDTD) method. The electric (E) and magnetic (H) field components are discretized using a central differencing scheme (second-order) in both space and time domains. The equations are solved using the leap-frog methodology; the electric field is solved at a given time step, the magnetic field is solved at the next time step, and the process is repeated sequentially. The fluid flow and heat transport within a porous medium are expressed through Eqs. (13)–(22). These equations are coupled to Maxwell's equations. These equations are solved numerically using a finite control volume approach along with the SIMPLE algorithm. The proposed discretization conserves the fluxes and avoids generation of a parasitic source. The basic strategy for the finite control volume discretization method is to divide the computational domain into a number of control volumes and then integrate the conservation equations over this control volume within an interval of time $[t, t+\Delta t]$. At the boundaries of the computational domain, integrating over half the control volume and taking into account the boundary conditions discretizes the conservation equations and at the corners a quarter of the control volume is utilized. The fully implicit time discretization finite difference scheme is used to arrive at the solution in time. To insure stability of the time-stepping algorithm Δt is chosen to satisfy the courant stability condition.

$$\Delta t\leqslant\frac{\sqrt{(\Delta x)^2+(\Delta y)^2}}{c} \tag{24}$$

and the spatial resolution of each cell satisfies:

$$\Delta x,\ \Delta y\leqslant\frac{\lambda_\mathrm{g}}{10\sqrt{\gamma_\mathrm{r}}} \tag{25}$$

where λ_g is the wavelength of microwave in the rectangular waveguide and γ_r is the relative electric permittivity.

The following set of simulation parameters are used to satisfy conditions given by Eqs. (24) and (25):

(1) Grid size: $\Delta x = 1.0$ mm and $\Delta y = 1.0$ mm.
(2) Time steps: $\Delta t = 2\times10^{-12}$ s is used corresponding to electromagnetic field and $\Delta t = 0.01$ is used corresponding to temperature field, velocity field and concentration calculations.
(3) Relative error in the iteration procedures is ensured to be less than 10^{-6}.

4. Results and discussions

4.1. Validation

The computational results are displayed in Fig. 2. The results are in excellent agreement with the results given by Klinbun [13]. This model can be used to describe the fundamental attributes of forced convection in a porous medium subject to an imposed electromagnetic field.

In order to verify the accuracy of the present model, the numerical results for the case without concentration transport are validated against the analytical results under the same conditions as obtained by Klinbun [13].

Overall, the results of the present study are in excellent agreement with the analytical results obtained by Klinbun [13]. This highly favourable comparison lends confidence to the accuracy of the present numerical model.

4.2. Analysis of electromagnetic field

Fig. 3 shows a simulation of an electric field at a microwave frequency of 2.45 GHz, microwave power of 500 W, Particle Reynolds number $(\mathrm{Re_p} = \rho_f u_e d_p/\mu) = 0.1$, where the centre of the porous media can be seen that large amplitude and gradually decreases as the wave moves into the porous media. Most waves are reflected back from the surface and show resonance with a large amplitude, while the electric field in the material gradually decreases and disappears because of the wave penetration.

4.3. The influence of microwave power on the distribution of temperature, velocity, and concentration of fluid in porous media

4.3.1. Distribution of temperature

Related to the problem of the process of heat from the microwave that is related to the electromagnetic field and the distribution of the temperature. This study estimates the electromagnetic field, which indicates the power of the microwaves inside the dielectric materials and also indicates that the power gradually decreased. This means that the power of the wave is changed into another form that we call heat. In other words, the power of the microwaves decreases slightly, because it has been absorbed by the dielectric materials and the wave has been changed into the heat form, which is called internal heat generation. In contrast, the properties of the electric materials have a large effect on the

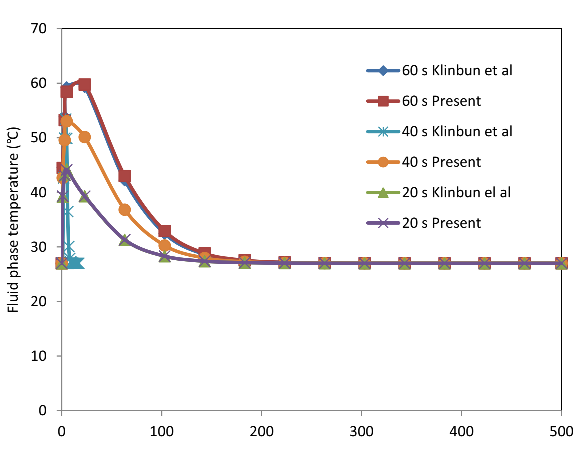

Fig. 2. Comparisons of fluid phase temperature for the present work versus the results of Klinbun et al.

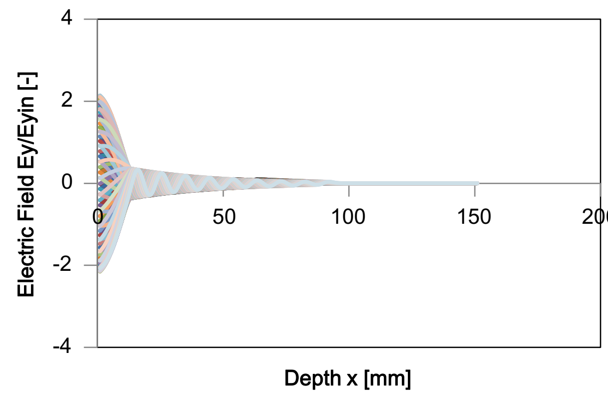

Fig. 3. Simulation of the electric field along porous packed bed at microwave frequency of 2.45 GHz, microwave power of 500 W Reynolds number $(\mathrm{Re_p}) = 0.1$, inlet concentration $(C_{in}) = 30\ \mathrm{mol/dm^3}$.

microwaves by dropping off the power generator of the microwave.

Figs. 4 and 5 display the effect of variations in the microwave power on the distribution of temperature. The results show that the highest temperatures values correspond to the highest microwave power. The highest temperature values for the cases considered here correspond to a microwave power of 1600 W, while a microwave power of 800 W produces the lowest values of the temperature. Since the power of the microwave is more intense than the electromagnetic field, the materials can absorb a huge energy from the microwave power. The most absorption occurs at the middle of the porous media, because of the high density of the electromagnetic field around the centre of the porous media, which gives this area the highest temperature. The distribution of temperature happens on the left side that takes the microwave wave has a high temperature, which slowly decreases along the x-axis. From the figure, it can be seen that the upper boundary of the distribution of temperature is higher than the lower boundary because this study specified that the upper boundary has the high temperature.

To classify the outcome on qualitative ratings for the LTE assumption, this may be expressed in the following form

$$\%\ \mathrm{LTE} = \left(\frac{T_{f(i,j)} - T_{s(i,j)}}{T_{f(i,j)}}\right) \times 100 \tag{26}$$

Comparing the distribution of temperature on the x and y axis at 60 s, the left side obviously has high temperature and gradually down along the depth. After all, the mechanism process of the high absorption of porous media as we called High Lossy Material. Most of the waves incident on the material are always absorbed by the porous media, except for those that are reflected out to the surface. Also, the waves that are transmitted through the layer of the porous media are less.

Fig. 6 compares the percentage difference between the distributions of temperature of the fluid phase and the solid phase at 0–60 s at 25 mm on the x-axis, and 99 mm on y-axis, at a microwave frequency of 2.45 GHz and microwave powers of 500, 800, 1000 and 1600 W. At the time of 10 s, it can be seen that the percentage difference in the distributions of temperature of the fluid phase and solid phase is highest at the microwave power of 1600 W (% LTE = 14). At microwave powers of 500, 800, and 1000 W, the% LTE is 3–8. As can be seen, the assumption of local thermal equilibrium deteriorates as the microwave power increase. The local thermal equilibrium assumption is suitable in the case of a microwave power of 1600 W.

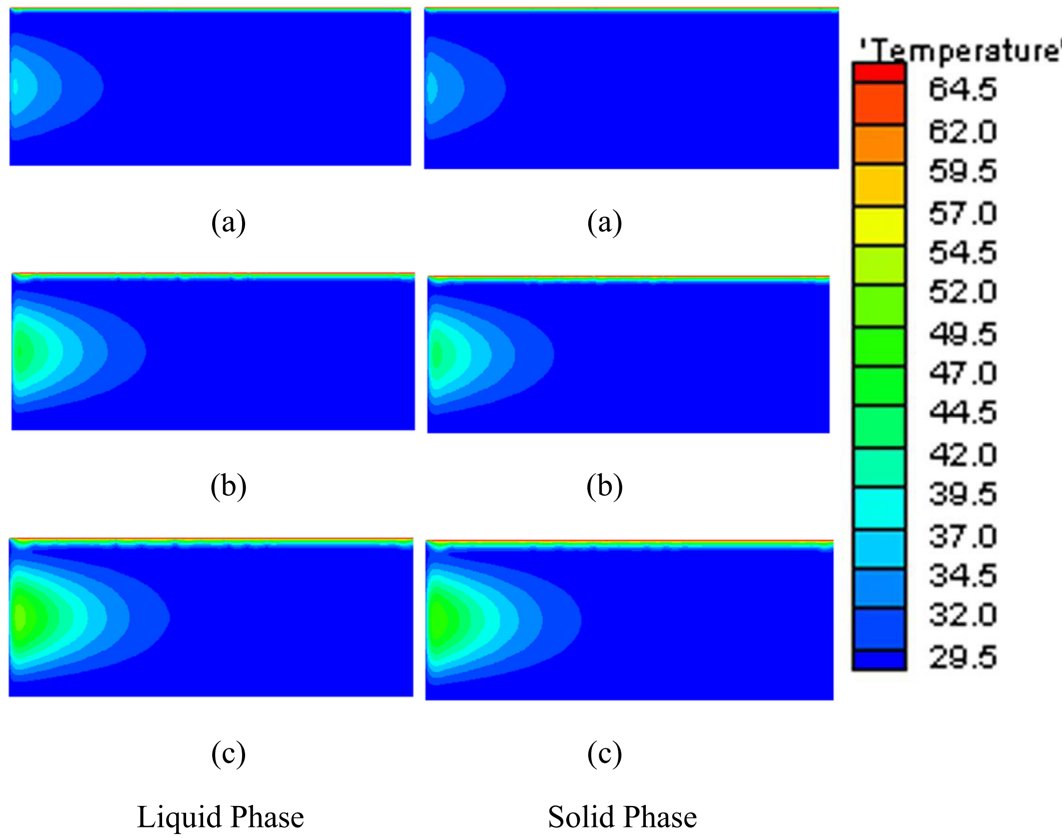

Fig. 4. Distribution of temperature in porous media (°C) with elapsed times: (a) 20 s (b) 40 s (c) 60 s at microwave power of 800 W (microwave frequency of 2.45 GHz, Reynolds number (Re_p) = 0.1, inlet concentration (C_{in}) = 30 mol/dm^3).

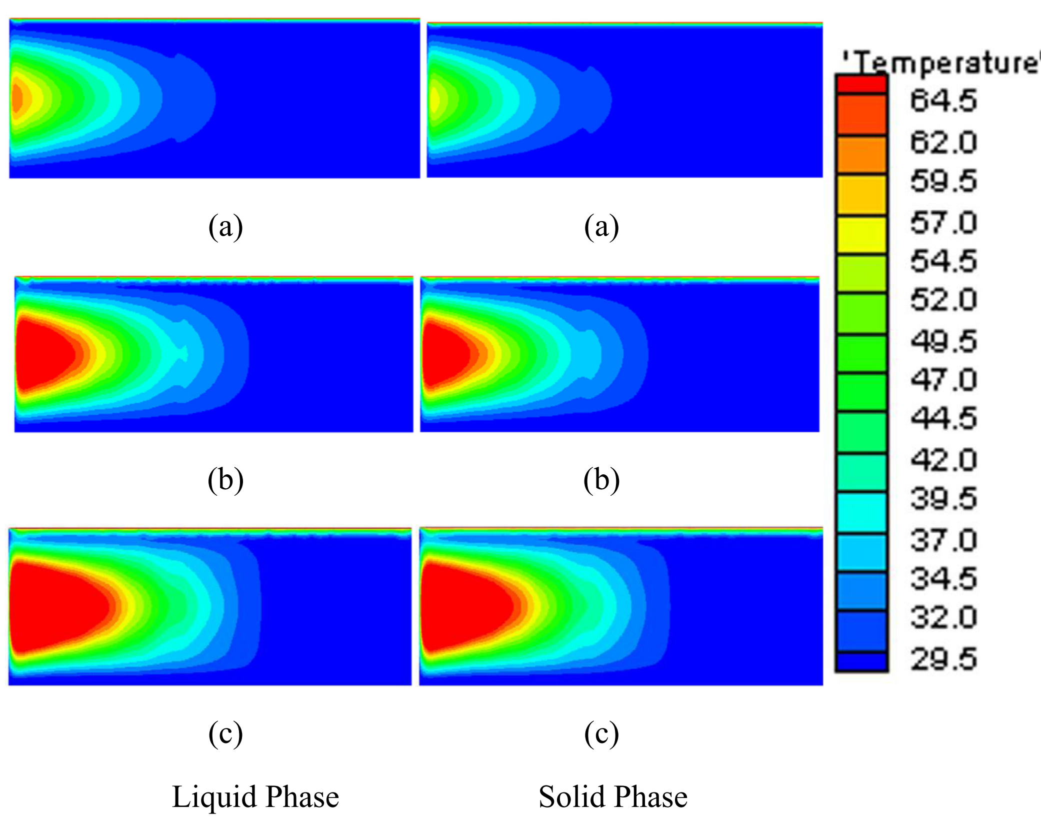

Fig. 5. Distribution of temperature in porous media (°C) with elapsed times: (a) 20 s (b) 40 s (c) 60 s at microwave power of 1600 W (microwave frequency of 2.45 GHz, Reynolds number (Re_p) = 0.1, inlet concentration (C_{in}) = 30 mol/dm^3).

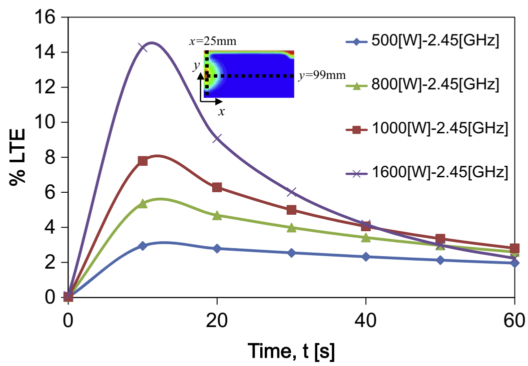

Fig. 6. Percent difference of distribution of temperature of solid and fluid phase at x-axis = 25 mm, y-axis = 99 mm at different microwave power with elapsed times (microwave frequency of 2.45 GHz, inlet concentration (C_{in}) = 30 mol/dm^3).

Fig. 7 shows the relationship of the temperature of the fluid and solid phases at operating inlet microwave powers of P = 500, 800, 1000, 1600 W at 99 mm on the y-axis, and frequency of 2.45 GHz at 60 s. The temperature increased and reached a maximum at about 25 mm on x-axis and then gradually decreased along the x-axis. The temperature decreases in the direction of the wave, which is consistent with the conditions of resonance of a standing wave. The microwave energy is changed into heat energy in the porous media. The maximum temperatures in the porous media are approximately 40, 51, 63, and 97 °C at values of microwave power of 500, 800, 1000, and 1600 W, respectively at a microwave frequency of 2.45 GHz.

This study proves the distribution of temperature in the porous media; in the case of higher power, there is a higher distribution of temperature. The middle of the porous has a constant distribution of temperature. The influence of the fluid (Marangoni effect) makes the heat move from the middle to the surrounding surface. Including, this figure also shows that the temperature inside the porous media increases slightly at the beginning of the heating process. After that, the temperature gradually decreases because the action of the dielectric loss factor decreases when the temperature increases.

4.3.2. Flow pattern

Velocity fields within the porous media at t = 60 s are discussed, and it can be seen that the microwave power has an important effects on the velocity field. This study investigates three values of powers, namely 500, 800, and 1600 W. The physical data are

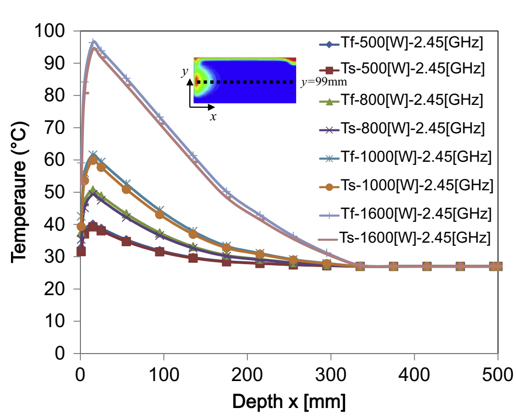

Fig. 7. Distribution of temperature of the solid and fluid phase at difference microwave power along x-axis at y-axis = 99 mm (microwave frequency of 2.45 GHz at time 60 s inlet concentration (C_{in}) = 30 mol/dm^3).

f = 2.45 GHz, Re_p = 0.1, and C_{in} = 0.3 mol/l. Figs. 8 and 9 show the flow field inside the porous media when the porous media is inserted in the waveguide during microwave heating with operating powers of 800 and 1600 W, respectively. Fluid flow fields are in the same direction but the magnitudes of velocity are clearly different: in the case of a microwave power of 1600 W, the density of the electric field in the porous media is higher than in the case of a microwave power of 800 W. The upstream region has strong velocity fields, because the upper layer of the porous media receives a strong incident wave. The vectors are rigorous near the upper right corner of the porous media and the velocity fields have a trend corresponding to the distribution of temperature.

The velocity vector has moved from the left because the difference in temperature between the left and the right parts of the porous media, leads to a difference in density. The volumetric expansion of the fluid and the buoyancy force driving the fluid motion are shown. In figure, the upper boundary of the distribution of velocity is similar to the distribution of temperature due to set on the edge of the area with high temperatures. The difference in temperature causes the velocity vector to move away from this position.

Figs. 8 and 9, flow field explains more of the process: at the very beginning of heating, the flow field has less influence on the heat convection but more influence on heat conduction. As the time increases, the difference between the surfaces of the porous media makes the process become convection fluid. Therefore, the fluid flow moves from the heated area to the cooler surrounding surface. This situation becomes the incidence that the heat convection process is very important in this procedure.

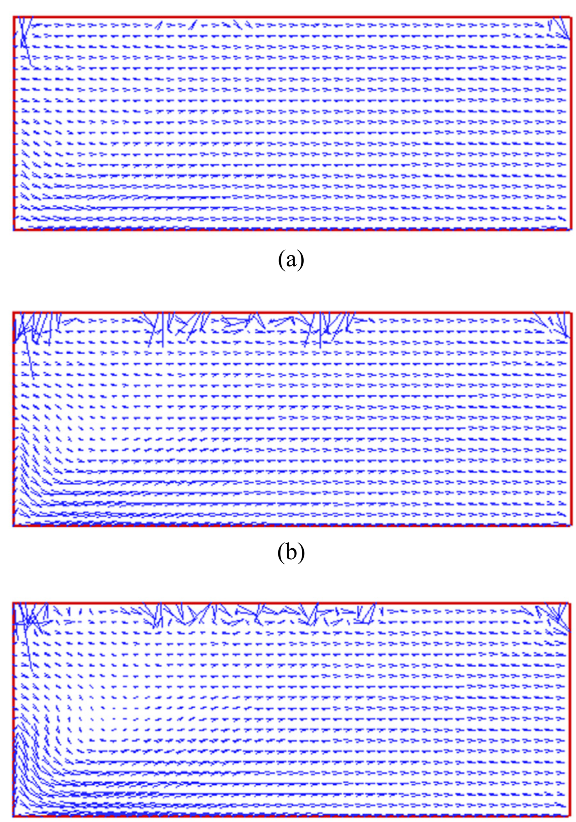

(a)

(b)

(c)

Fig. 8. Flow field with elapsed times: (a) 20 s (b) 40 s (c) 60 s at microwave power of 800 W (microwave frequency of 2.45 GHz, Re_p = 0.1, inlet concentration (C_{in}) = 30 mol/dm^3).

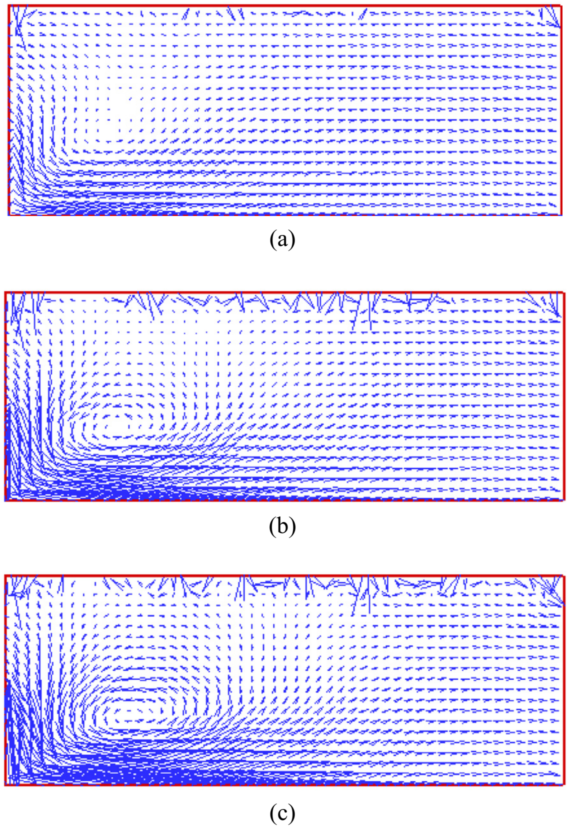

Fig. 9. Flow field with elapsed times: (a) 20 s (b) 40 s (c) 60 s at microwave power of 1600 W (microwave frequency of 2.45 GHz, $Re_p = 0.1$, inlet concentration (C_{in}) = 30 mol/dm^3).

4.3.3. Distribution of concentration

Fig. 1 shows a schematic diagram of the problem under consideration, from which it can be determined that has a higher concentration than the downward, and then the diffusion expands from the high to the low of the concentration. Considering the spread of the concentration from the left to the right of the porous media when fluid is input on the left, the concentration of the fluid decreases slowly until it is constantly at 55 mm and is maximal at the top and right of the porous media at 500 mm on the x-axis and 199 mm on the y-axis. Therefore, it shows the distribution of the concentration at 199 mm (y-axis).

The distributions of concentration within the porous media at an elapsed time of 60 s at microwave powers of 800 and 1600 W and a microwave frequency of 2.45 GHz are listed in Table 2. At the microwave power of 1600 W, is distributed higher concentration; for example, at 455 mm on the x-axis at an elapsed time of 60 s and microwave powers of 1600 and 800 W, concentrations of 9.00171 and 9.00130 mol/dm^3 are found with respect to the high microwave power and high density of the electric field. In the case of microwave power of 1600 W, the diffusion rate of concentration is better than in the case of microwave power of 800 W. The distribution of concentration is caused by diffusion, with the movement of solutes from areas of high concentration to areas of low concentration, and the movement stops when the concentration reaches equilibrium.

Table 2
Distribution of concentration with elapsed time 60 s at difference microwave power in the range of y-axis is 199 mm Reynolds number (Re_p) = 0.1, inlet concentration (C_{in}) = 30 mol/dm^3.

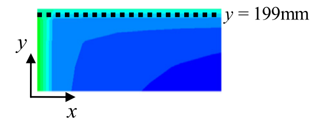

x-axis (mm)	Concentration of fluid at 60 s (mol/dm^3)	
	f2.45/P800	f2.45/P1600
1	9.61965	9.62001
5	8.97575	8.97792
15	8.77418	8.77020
55	8.63806	8.64581
95	8.63620	8.64615
135	8.63887	8.64771
175	8.63998	8.64618
215	8.64015	8.64402
255	8.64033	8.64189
295	8.64068	8.63898
335	8.64193	8.64424
375	8.64355	8.64473
415	8.68535	8.68609
455	9.00130	9.00171
495	12.44990	12.44996
500	13.55696	13.55693

4.4. The influence of inlet velocity on the distribution of temperature, velocity and concentration of fluids in the porous media

4.4.1. Distribution of temperature

The distribution of temperature within the porous media at operating inlet velocities of $Re_p = 0.5$ and 10 is displayed in Figs. 10 and 11, respectively. It seems that $Re_p = 10$ expands the distribution of temperature further because water is fed in at a higher speed.

4.4.2. Flow pattern

The velocity fields within the porous media at operating inlet velocities of $Re_p = 0.1$, 0.5, and 10 are displayed in Fig. 12(a)–(c), respectively. The velocity fields are in the same direction but the magnitudes of velocity are clearly different. Fig. 12(a) clearly displays the magnitude of velocity because the effect of the electromagnetic wave and natural convection is greater. Fig. 12(c) displays the flow cell at the upstream and downstream parts are absolutely because the inlet velocity overcomes effect of the electromagnetic field and natural convection.

Table 1
Thermal and dielectric properties used in the computations [13].

Material property	Air	Water	Soda lime
Density, ρ (kg m^{-3})	1.1	989	2225
Specific heat, C_p (J kg^{-1} K^{-1})	1008	4180	835
Thermal conductivity, k (W m^{-1} K^{-1})	0.028	0.640	1.4
Viscosity, μ (kg m^{-1} s^{-1}) $\times 10^5$	1.9	57.7	-
Dielectric constant, γ_r	1.0	$88.15 - 0.414T + (0.131 \times 10^{-2})T^2 - (0.046 \times 10^{-4})T^3$	7.5
Loss tangent, $\tan\delta$	0.0	$0.323 - (9.499 \times 10^{-3})T + (1.27 \times 10^{-4})T^2 - (6.13 \times 10^{-7})T^3$	0.0125

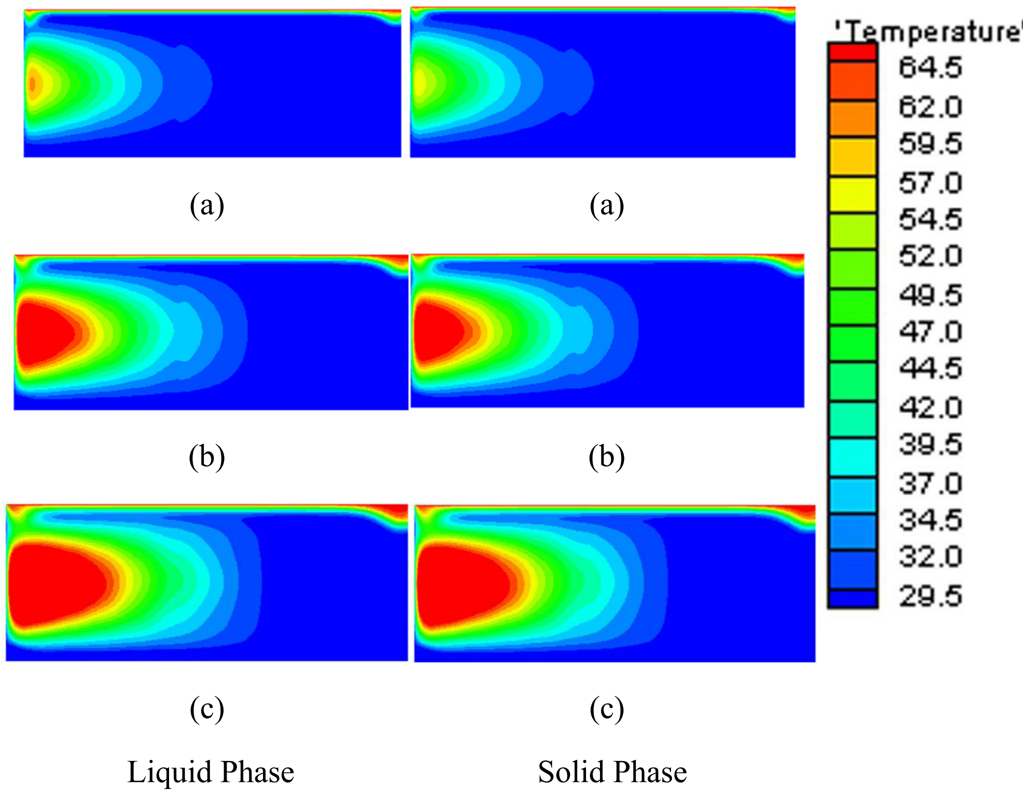

Fig. 10. Distribution of temperature in porous media (°C) with elapsed times: (a) 20 s (b) 40 s (c) 60 s at Reynolds number (Re_p) = 0.5 (microwave frequency of 2.45 GHz, microwave power of 1600 W, inlet concentration (C_{in}) = 30 mol/dm^3).

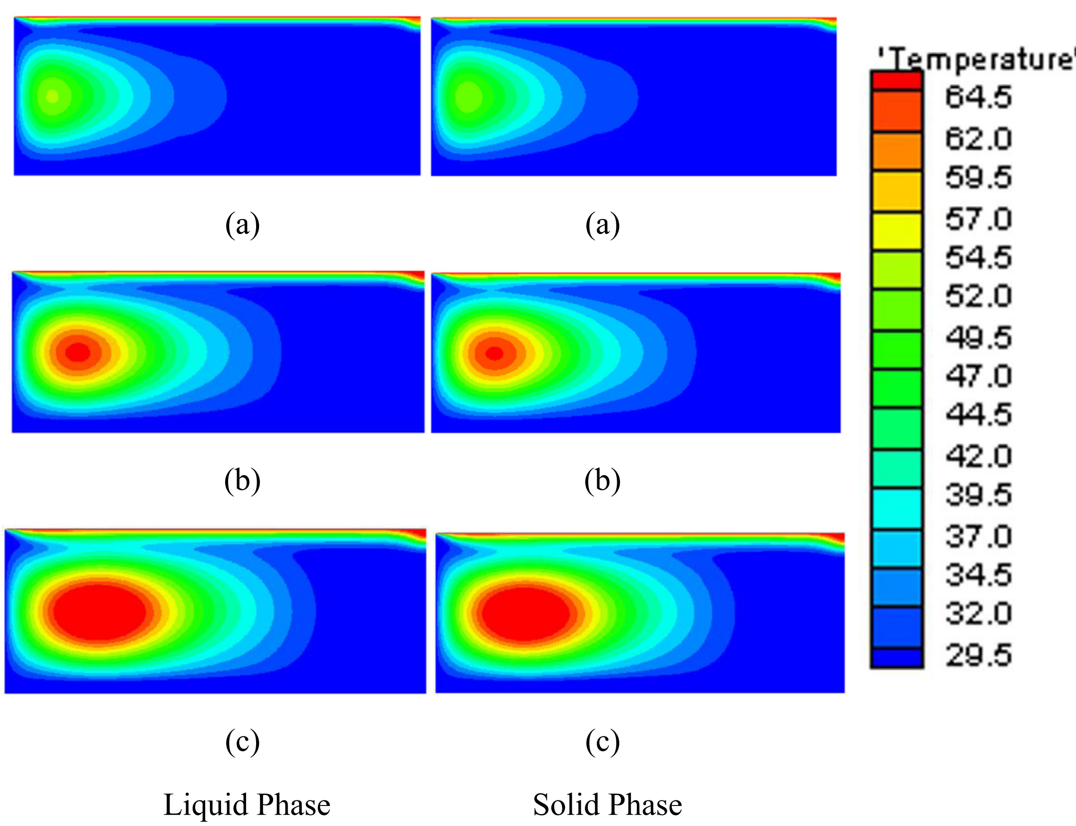

Fig. 11. Distribution of temperature in porous media (°C) with elapsed times: (a) 20 s (b) 40 s (c) 60 s at Reynolds number (Re_p) = 10 (microwave frequency of 2.45 GHz, microwave power of 1600 W, concentration (C_{in}) = 30 mol/dm^3).

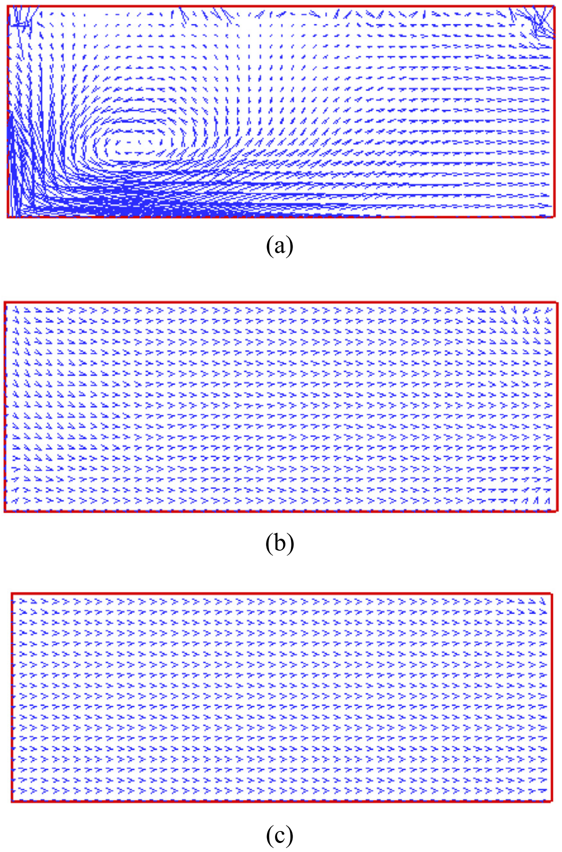

Fig. 12. Flow field with elapsed time 60 s at Reynolds number (Re_p): (a) 0.1 (b) 0.5 (c) 10 (microwave frequency of 2.45 GHz, microwave power of 1600 W, inlet concentration (C_{in}) = 30 mol/dm^3).

Table 3
Distribution of concentration elapsed time 60 s at Reynolds number (Re_p) = 0.1, 0.5, 10 (microwave frequency of 2.45 GHz, microwave power of 1600 W, concentration (C_{in}) = 30 mol/dm^3, y-axis is 199 mm).

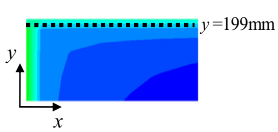

x-axis (mm)	Concentration of fluid at 60 s (mol/dm^3)		
	$Re_p = 0.1$	$Re_p = 0.5$	$Re_p = 10$
1	9.62001	11.59102	23.90462
5	8.97792	9.21239	16.44801
15	8.77020	8.76842	8.01331
55	8.64581	8.61002	7.89893
95	8.64615	8.60577	7.87235
135	8.64771	8.60721	7.87485
175	8.64618	8.60589	7.87882
215	8.64402	8.60377	7.88000
255	8.64189	8.60158	7.87990
295	8.63898	8.59872	7.87859
335	8.64424	8.60442	7.88114
375	8.64473	8.60648	7.88745
415	8.68609	8.64976	7.90925
455	9.00171	8.97866	8.14963
495	12.44996	12.44666	12.38851
500	13.55693	13.55896	13.64876

4.4.3. Distribution of concentration

The distributions of concentration within the porous media at operating inlet velocities of $Re_p = 0.1$, 0.5, and 10 are displayed in Table 3. It seems that the trend of the concentration of the fluid at 60 s decreases along the x-axis and gradually increases after 335 mm on the x-axis. At 455 mm on the x-axis, inlet velocities of $Re_p = 0.1$, 0.5, and 10 give concentrations of 9.00171, 8.97866, and 8.14963 mol/dm^3, respectively.

5. Conclusions

The effect of an electromagnetic field on transportation through a porous medium is analyzed in this research. The transient Maxwell's equations are utilized to describe the electromagnetic field distribution inside the waveguide and the porous medium while the flow field is simulated by using the Brinkman–Forchheimer and Darcy model. Furthermore, the extended concentration equation of the LTNE model is employed to express the heat transport phenomena in a porous medium.

The conclusions drawn from this work can be summarizes as follow:

The model was developed to describe the flow behavior, distribution of concentration, and distribution of temperature in a porous media. The magnitude of electromagnetic wave power has a substantial impact on the temperature of the porous media. An increase in the electromagnetic wave power produces a higher temperature of the porous media and causes a larger temperature difference between the solid and fluid phases. The high microwave power (1600 W) has the most influence on the distribution of temperature, flow fields, and distribution of concentration of the fluid within the porous media during saturated flow. The high inlet fluid velocity ($Re_p = 10$) has the most influence on the distribution of the temperature. During the application of high microwave power (1600 W), the LTNE model is suitable for testing this simulation. Our results show that an imposed electromagnetic field has a substantial effect on altering the LTE between the solid and fluid phases in a porous media.

Acknowledgements

The authors gratefully acknowledge the Thailand Research Fund (under the TRF contract No. RTA5980009 and PHD/0059/2557).

References

[1] K. Khanafer, K. Vafai, Double-diffusive mixed convection in a lid-driven enclosure filled with a fluid-saturated porous medium, Int. J. Comput. Methodol. 42 (5) (2002) 465–486.
[2] M. Karimi-Fard, M.C. Charrier-Mojtabi, K. Vafai, Non-Darcian effects on double-diffusive convection within a porous medium, Int. J. Comput. Methodol. 31 (8) (1997) 837–852.
[3] S.K. Jena, S.K. Mahapatra, A. Sarkar, Double diffusive buoyancy opposed natural convection in a porous cavity having partially active vertical walls, Int. J. Heat Mass Transfer 62 (1) (2013) 805–817.
[4] O.V. Trevisan, A. Bejan, Natural convection with combined heat and mass transfer buoyancy effects in a porous medium, Int. J. Heat Mass Transfer 28 (8) (August 1985) 1597–1611.
[5] T. Nishimura, M. Wakamatsu, A.M. Morega, Oscillatory double-diffusive convection in a rectangular enclosure with combined horizontal temperature and concentration gradients, Int. J. Heat Mass Transfer 41 (11) (June 1998) 1601–1611.
[6] J.A. Weaver, R. Viskanta, Natural convection in binary gases due to horizontal thermal and solutal gradients, J. Heat Transfer 113 (1) (February 1991) 141–147.
[7] P. Nithiarasu, K.N. Seetharamu, T. Sundararajan, Double-diffusive natural convection in an enclosure filled with fluid-saturated porous medium: A generalized non-Darcy approach, Numer. Heat Transfer, Part A: Appl. 30 (4) (1996) 413–426.
[8] C. Saltiel, A. Datta, Heat and mass transfer in microwave processing, Adv. Heat Transfer 33 (1999) 1–94.
[9] T. Wessapan, P. Rattanadecho, Influence of ambient temperature on heat transfer in the human eye during exposure to electromagnetic fields at 900 MHz, Int. J. Heat Mass Transfer 70 (2014) 378–388.
[10] W. Cha-um, P. Rattanadecho, W. Pakdee, Experimental analysis of microwave heating of dielectric materials using a rectangular wave guide (Mode: TE_{10})

(Case study: water layer and saturated porous medium), Exp. Thermal Fluid Sci. 33 (3) (2009) 472–481.
[11] W. Klinbun, P. Rattanadecho, W. Pakdee, Microwave heating of saturated packed bed using a rectangular waveguide (TE_{10} mode): Influence of particle size sample dimension, frequency and placement inside the guide, Int. J. Heat Mass Transfer 54 (2011) 1763–1774.
[12] P. Keangin, P. Rattanadecho, Analysis of heat transport on local thermal non-equilibrium in porous liver during microwave ablation, Int. J. Heat Mass Transfer 67 (2013) 46–60.
[13] W. Klinbun, K. Vafai, P. Rattanadecho, Electromagnetic field effects on transport through porous media, Int. J. Heat Mass Transfer 55 (1–3) (January 2012) 325–335.
[14] A. Nakayama, F. Kuwahara, M. Sugiyama, G. Xu, A two-energy equation model for conduction and convection in porous media, Int. J. Heat Mass Transfer 44 (2001) 4375–4379.
[15] M. Quintard, Modelling local thermal non-equilibrium heat transfer in porous media, Proceedings of the Eleventh International Heat Transfer Conference, vol. 1, 1998, pp. 279–285.
[16] A. Amiri, K. Vafai, Analysis of dispersion effects and non-thermal equilibrium, non-Darcian, variable porosity incompressible flow through porous media, Int. J. Heat Mass Transfer 37 (1994) 939–954.
[17] A.V. Kuznetzov, An analysis solution of heating a two-dimensional porous packed bed by a non-thermal equilibrium fluid flow, Appl. Sci. Res. 55 (1995) 83–93.
[18] G. Mur, Absorbing boundary conditions for the finite difference approximation of the time domain electromagnetic field equations, IEEE Trans. Electromagn. Compat. 23 (1981) 377–382.